# A Model of 'Disparitions Brusques'
## (sudden disappearance of eruptive prominences)
## As an Instability Driven by MHD Waves

Jun-ichi SAKAI

Department of Applied Mathematics and Physics, Faculty of Engineering, Toyama University, Takaoka, Toyama 933, Japan.

and

Ken-Ichi NISHIKAWA

Plasma Physics Laboratory, Princeton University, Princeton, New Jersey, 08540 U.S.A.

**ABSTRACT**

A model of 'disparitions brusques' (sudden disappearance of eruptive prominences) is discussed based on the Kippenhahn and Schlüter configuration. It is shown that Kippenhahn and Schlüter's current sheet is very weakly unstable against magnetic reconnecting modes during the lifetime of quiescent prominences. Disturbances in the form of fast magnetosonic waves originating from nearby active regions or the changes of whole magnetic configuration due to newly emerged magnetic flux may trigger a rapidly growing instability associated with magnetic field reconnection. This instability gives rise to disruptions of quiescent prominences and also generates high energy particles.

## I. INTRODUCTION

It is well known that quiescent prominences are long-lived, slowly changing phenomena with lifetimes ranging from days to months, and which sometimes undergo a sudden disappearance due to an ascending motion which is called as 'disparitions brusques' (see Tandberg-Hanssen, 1974). Their dimensions are generally taken to be of the order of $5 \times 10^3$ km wide, $5 \times 10^4$ km high, and $10^5$ km long. The characteristic temperature is of the order of $5 \times 10^3$ K and the electron number density is in the range of $10^{10} - 10^{11}$ cm$^{-3}$. The magnetic field is not as yet directly measurable, but limb observations give a line of sight magnetic field $B_{11}$ which is in the range of 0.5 to 30 or 40 gauss (Tandberg-Hanssen, 1974).

The cause of disparitions brusques generally is a flare-induced activation and here the external perturbations have a profound influence on the stability of quiescent prominences. Some temporary disturbances seem to trigger an instability which causes the disparition brusque.

Skylab observations have shown that the filament disruptions represent one of the most important mechanisms of solar activity (see Švestka, 1989). Soft X-rays pictures show a brightening

above the place where the filament just disappeared (Švestka, 1976, p. 230), which means that there occur plasma heating and particle acceleration.

The filament activation has been discussed in connection with the two-ribbon flare. After the disparition brusque, X-rays pictures show that a system of growing loops has maximum brightness at their tops, where the temperature exceeds $10^7$ K (Švestka, 1980). This loop system grows and at the same time the two ribbons drift apart at the loop foot points (Švestka, 1976, Fig. 6). Hyder (1967) has presented a phenomenological model for disparitions brusques based on the Kippenhahn and Schulüter model (1957) and the Dungey model (1958). For a comprehensive review of prominences and models the reader is referred to Tandberg-Hanssen's book (1974).

Since the Kippenhahn and Schlüter model, several attempts of explaining the structure of quiescent prominences have been made (Low, 1975 ; Lerche and Low, 1977 ; Heasley and Mihalas, 1976 ; Milne, Priest and Roberts, 1979 ; Low and Wu, 1981) by the combination of magneto-statics and energetics.

On the other hand, the problem of the stability of quiescent prominences has been attacked by several authors (Kuperus and Tandberg-Hanssen, 1967 ; Anzer, 1969 ; Nakagawa and Malville, 1969 ; Nakagawa, 1970 ; Pustil'nik, 1974 ; Dolginov and Ostryakov, 1980 ; also see Tandberg-Hanssen's book, 1974). However, the triggering mechanisms causing disparitions brusques are still not clear.

In the present paper we propose a model of disparitions brusques as an instability externally driven by MHD waves, based on the Kippenhahn and Schlüter equilibrium model which is generally accepted. Except for the Rayleigh-Taylor instability which may be important for limiting the size of prominence (Dolginov and Ostryakov, 1980), the Kippenhahn and Schlüter configuration is stable against ideal MHD perturbations with $k \cdot g = 0$ (Miglivalo, 1982) as well as $k \| g$ (Zweibel, 1982). In Sec. II, we present the stability analysis for resistive MHD perturbations, especially magnetic reconnecting modes which may be important for the explanation of plasma heating and particle acceleration processes observed after disparition brusque. It is shown that the Kippenhahn and Schlüter's current sheet is very weakly unstable against magnetic reconnecting modes during the lifetime of quiescent prominences.

In Sec. III we discuss some temporary disturbances such as fast magnetosonic waves originating from nearby active regions or the changes of whole magnetic configuration due to a newly emerged magnetic flux nearby. We show that these disturbances may trigger a rapid growing instability associated with magnetic field reconnection. It is shown that the ponderomotive force due to finite amplitude fast magnetosonic waves can induce an effective ascending motion which in turn causes a rapid growing instability with broad band fluctuations. In Sec. IV we discuss some nonlinear effects associated with reconnecting modes and suggest the plasma heating and particle acceleration mechanisms.

## II. STABILITY OF KIPPENHAHN AND SCHLÜTER MODEL AGAINST RECONNECTING MODES

### II-1, Kippenhahn and Schlüter Model

We briefly review the Kippenhahn and Schlüter model, which is a most simple analytic model. A dense plasma sheet in the corona against gravity is supported by the magnetic tension

(Fig. 1). The solution can be obtained from the static equilibrium equation,

$$\nabla p_0 - \rho_0 g e_x - \frac{1}{4\pi}\mathrm{curl}\, \boldsymbol{B}_0 \times \boldsymbol{B}_0 = 0\,, \quad (2\text{-}1)$$

and the equation of state,

$$p_0 = n_0 \varkappa T_0\,, \quad (2\text{-}1)$$

where $\rho_0$ is the density, $p_0$ the pressure, $B_0$ the magnetic field, $n_0$ the number density, $T_0$ the temperature and $\varkappa$ Boltzman constant. The magnetic field and density distribution are given by the following relations,

$$B_{x0}(y) = B_\infty \tanh(y/a)\,, \quad (2\text{-}3)$$

$$B_{y0} = B_n = \text{const.}\,, \quad (2\text{-}4)$$

$$\rho_0(y) = \rho(0)\,\mathrm{sech}^2(y/a), \quad (2\text{-}5)$$

where a is the characteristic width of the prominence, $B_\infty$ the magnetic field component far from the sheet, $\rho(0)$ the density at $y=0$ (Fig. 2(a)). From the force balance in the $x$ direction, we have

$$E_n = \frac{B_n}{B_\infty} = \frac{ag}{2c_s^2}\,, \quad (2\text{-}6)$$

where $c_s$ is the sound velocity (temperature is assumed to be constant), and $E_n$ shows the measure of relative strength between $B_x$ and $B_y$. In the corona, $E_n$ is in the range of 1-10, if we use $a \sim 5.10^3$ km, $g \sim 10^4$ cms$^{-2}$ and $T_0 \sim 5 \times 10^3$ K.

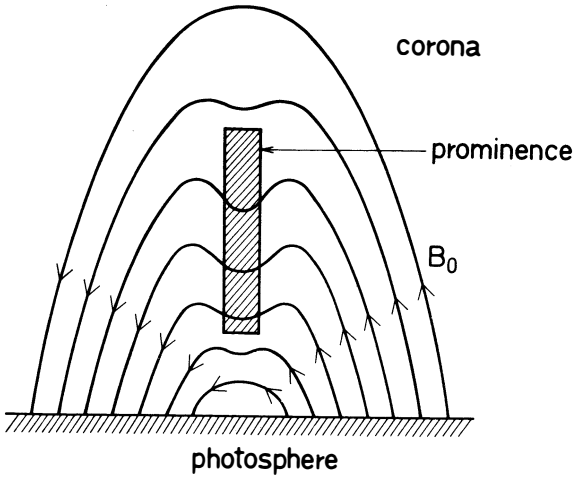


Fig. 1 A schematic configuration of a quiescent prominence based on Kippenhahn and Schlüter model.

## II-2. Reconnecting Modes

We investigate the stability of the current sheet shown in Fig. 2(a) against reconnecting modes, namely current filamentation instability in which magnetic field disturbances are schematically drawn in Fig. 2(b). This reconnecting mode has been treated (Nishikawa and Sakai, 1982) in connection with tearing modes (Furth, Killeen and Rosenbluth, 1963), because in the limit of $E_n \to 0$, the Kippenhahn and Schlüter

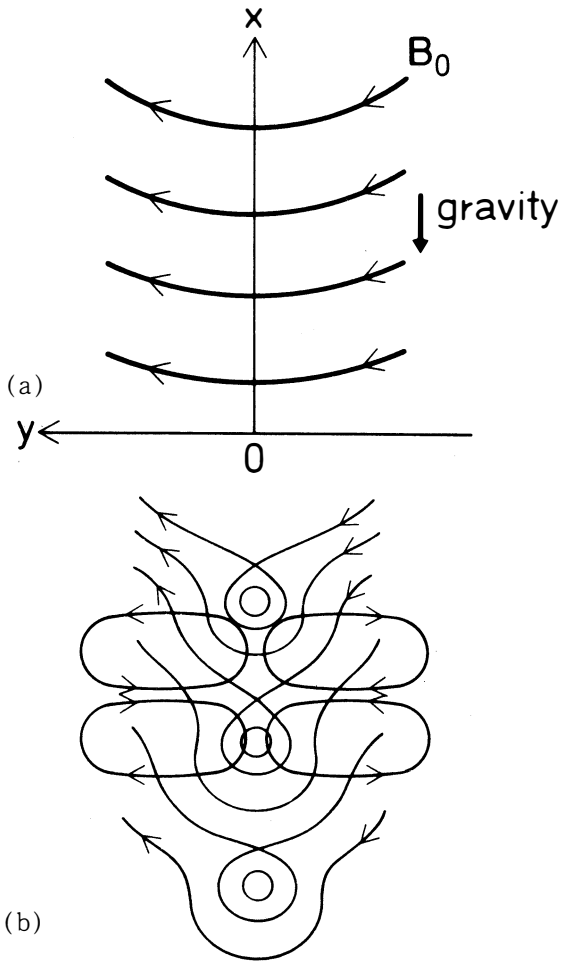


Fig. 2 Magnetic field configurations. (a) The equilibrium state. (b) Reconnecting modes and vortex motions.

configuration becomes an ideal neutral current sheet with completely anti-parallel magnetic field.

We present basic MHD equations including gravity,

$$\frac{\partial \rho}{\partial t} + \mathrm{div}(\rho \boldsymbol{v}) = 0, \tag{2-7}$$

$$\rho\left(\frac{\partial \boldsymbol{v}}{\partial t} + \boldsymbol{v}\cdot\nabla\boldsymbol{v}\right) = -\nabla p + \frac{1}{4\pi}\,\mathrm{curl}\,\boldsymbol{B}\times\boldsymbol{B} - \rho g e_x, \tag{2-8}$$

$$\frac{\partial \boldsymbol{B}}{\partial t} = \mathrm{curl}(\boldsymbol{v}\times\boldsymbol{B}) + \frac{c^2}{4\pi\sigma}\nabla\boldsymbol{B}, \tag{2-9}$$

where the pressure is $p = \rho c_s^2$ and $\sigma$ the conductivity. The plasma is assumed to be incompressible, because the prominence plasma is low $\beta$. Introducing vector potentials $\phi$ and $A$ defined by $\boldsymbol{v} = \mathrm{curl}\,\phi e_z$ and $\boldsymbol{B} = \mathrm{curl}\,A e_z$, and furthermore linearizing Eqs. (2-7)-(2-9) around the equilibrium solutions of Eqs. (2-3)-(2-5) lead to the following system of equations,

$$\frac{\partial \rho_1}{\partial t} - \frac{\partial \phi}{\partial x}\frac{d\rho_0}{dy} = 0, \tag{2-10}$$

$$\frac{\partial}{\partial t}\left[\frac{\partial}{\partial x}\left(\rho_0\frac{\partial \phi}{\partial x}\right) + \frac{\partial}{\partial y}\left(\rho_0\frac{\partial \phi}{\partial y}\right)\right] - \frac{1}{4\pi}\left[B_{x0}\Delta\left(\frac{\partial A}{\partial x}\right) - \frac{d^2B_{x0}}{dy^2}\frac{\partial A}{\partial x} + B_n\,\Delta\frac{\partial A}{\partial y}\right]$$

$$+ g\frac{\partial \rho_1}{\partial y} = 0, \tag{2-11}$$

$$\frac{\partial A}{\partial t} = B_n\frac{\partial \phi}{\partial y} + B_{x0}\frac{\partial \phi}{\partial x} + \frac{c^2}{4\pi\sigma}\Delta A, \tag{2-12}$$

where Eq. (2-11) can be derived from the $z$ component of the curl of Eq. (2-8) and Eq. (2-12) is the $x$ component of Eq. (2-9). The last term $g\frac{\partial \rho_1}{\partial y}$ in Eq. (2-11) gives rise to an effective acceleration on disturbances which leads to strong stabilization on reconnecting modes. Taking $B_n \to 0$, these equations reduce to those derived by Furth et al. (1963). We assume that all physical quantities vary like $f(y)\exp[i(kx - \omega t)]$ and we normalize these quantities as follows: $\rho, \phi, A, y$, and $t$ by $\rho(0)$, $v_A a$, $aB_\infty$, a and $\tau_A$, respectively, where $v_A = B_\infty/\{4\pi\rho(0)\}^{1/2}$ and $\tau_A = a/v_A$. After some manipulations, we obtain

$$\frac{d^2A}{dy^2} = EA + F\frac{d\phi}{dy} + G\phi, \tag{2-13}$$

$$\frac{d^2\phi}{dy^2} = P\frac{d\phi}{dy} + Q\phi + R\frac{dA}{dy} + VA, \tag{2-14}$$

where coefficients are given by

$$E = \alpha^2 - iS\omega_0, \qquad F = -SE_n, \qquad G = -iS\alpha th(y),$$

$$P = \left\{\left[2th(y) + \frac{\alpha E_n}{\omega_0}sh(2y)\left[S - \frac{i}{\omega_0}\mathrm{sech}^2(y)\right]\right\}/T,\right.$$

$$Q = \left(\frac{\alpha}{\omega_0}\left\{SE_n + iS\alpha sh^2(y) - 2i\frac{E_n}{\omega_0}[1 - 3th^2(y)]\right\} + \alpha^2\right)/T, \tag{2-15}$$

$$R = SE_n ch^2(y)/T,$$

$$V = \alpha sh(2y)\left[iS/2 - \frac{1}{\omega_0}\mathrm{sech}^2(y)\right]/T,$$

$$T = 1 + i\frac{SE_n^2}{\omega_0} ch^2(y), \qquad \alpha = ka, \qquad \omega_0 = \omega\tau_A .$$

$S = \tau_R/\tau_A$ ($\tau_R = 4\pi\sigma a^2/c^2$) shows the magnetic Reynolds number which is the order of $10^7-10^8$ in the prominence. Alfvēn trasit time $\tau_A$ is 20 s and the resistive diffusion time $\tau_R$ is about $10^9$ s. The eigen-value equations, (2-13) and (2-14) have been solved for the even $A$ and odd $\phi$ mode (Fig. 3) which shows magnetic islands. The numerical procedure employed is referred to our previous work (Nishikawa, 1980).

The characteristics of the reconnecting mode are summarized as follows:

(1) As shown in Fig. 4, gravity, namely the normal magnetic field $B_n$ (see eq. (2-6)) has

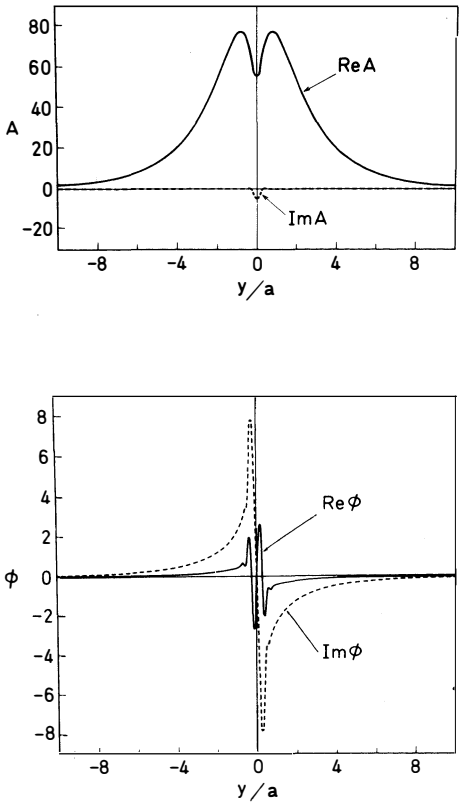


Fig. 3 Eigenmode structures of $A$ and $\phi$ with $S=10^3$, $E_n=B_n/B_\infty=0.01$, $ka=0.5$, and $\omega\tau_A = 0.001806 + 0.01049\,i$. The amplitudes of $A$ and $\phi$ are plotted in arbitrary units.

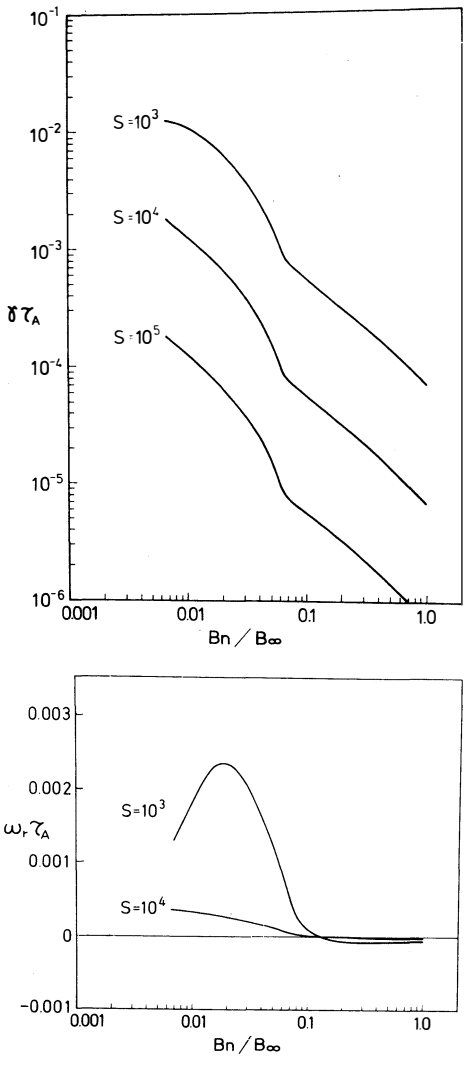


Fig. 4 Dependence of the eigenvalues on the values of $E_n=B_n/B_\infty$ with $ka=0.5$ and $S=10^3$, $10^4$, and $10^5$.

strong stabilization effect against the reconnecting mode. The growth rate $\gamma\tau_A$ is proportional to $S^{-1}$ for $E_n \gtrsim 0.1$ as compared to $\gamma\tau_A \propto S^{-3/5}$ for the classical collisional tearing mode. It is difficult to compute the growth rate in the range of $S \simeq 10^7$-$10^8$ for prominences, however, we find that the growth rate $\gamma\tau_A$ is the order of $10^{-7}$-$10^{-8}$ by the extrapolation of computational results. This growth time is close to the diffusion time $\tau_R \sim 10^9$ s, which means that the prominences are almost stable during their lifetime (several months $\simeq 10^7$ s).

(2) The growth rate versus wavenumber is shown in Fig. 5. The maximum growth rate occurs near $ka \simeq 0.2$. The reconnecting mode has a real frequency, which shows that the magnetic islands can propagate along the vertical direction of the prominence.

From these results, we conclude that the prominence based on Kippenhahn and Schlüter model is almost stable against the reconnecting mode.

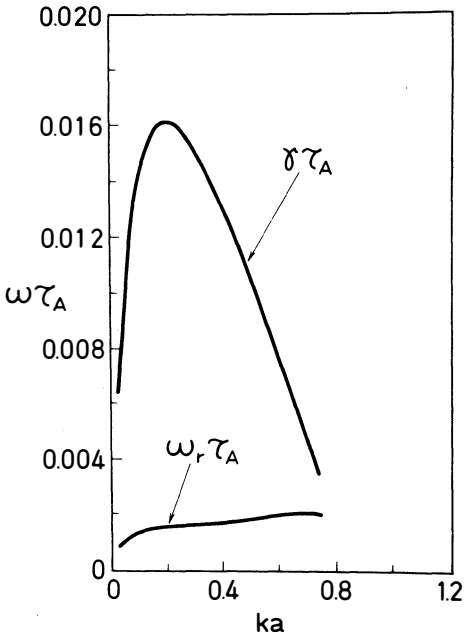


Fig. 5 Growth rate and real frequency as a function of $ka$ with $S = 10^3$ and $E_n = B_n/B_\infty = 0.01$.

## III. TRIGGERING MECHANISMS OF DISPARITIONS BRUSQUES

Observations indicate that the whole prominence rises in the atmosphere at a steady increasing velocity and disappears. Since the prominence often reforms in the same location and basically with the same shape, it is thought that the supporting magnetic field is not destroyed, merely temporarily disturbed. This temporary disturbances seem to trigger an instability which causes the disparition brusques. Some disturbances may originate from nearby active region or solar flares.

We propose two triggering mechanisms leading to ascending motion of prominences. One possibility is that if some disturbances may hit the foot magnetic field supporting the prominence, to increase the normal magnetic field $B_n$, the magnetic tension may exceed the gravity force and in turn, give rise to ascending motion. Another possibility considered here is the interaction between the reconnecting mode and fast magnetosonic waves originating from other active regions or solar flares.

We may imagine that the finite amplitude fast magnetosonic disturbances propagate vertically along the prominence, because in the prominence the main magnetic field is horizontal, i.e., ($B_n \gg B_{x0}$). If we consider fast modes with wavelengths, $\lambda_\perp$, which is smaller than the width, $a$, of the prominence ($\lambda_\perp \lesssim a$), it is a good approximation to neglect the diffraction effect due to inhomogeneity and also to treat fast modes propagating almost perpendicular to the normal magnetic field $B_n$.

### Ⅲ-1. Ponderomotive Force due to Fast Magnetosonic Waves

We consider nonlinear fast magnetosonic waves propagating upward in the prominence. Recently, the ponderomotive force due to fast waves has received much attention, because it can produce plasma vortex motions and excite forced tearing modes and ballooning modes (Sakai and Washimi, 1982; Sakai, 1982 (a)). The ponderomotive force due to fast waves (sakai and Washimi, 1982) is given by

$$F_x = -\rho_0 v_A^2 \frac{\partial I}{\partial x}, \tag{3-1}$$

$$F_y = \rho_0 v_A^2 \frac{\partial I}{\partial y}, \tag{3-2}$$

where $I$ denotes the wave intensity of the fast waves, $I = |\psi|^2 = (\Delta B/B_0)^2$. The sign of the $y$ component of the force means that it acts as a negative pressure, while the x component acts as an usual pressure. From the fact that curl $\boldsymbol{F} \neq 0$, we can conclude that the ponderomotive force creates plasma vortex motions which may enhance the weakly unstable reconnecting modes in the prominence. If we take into account the ponderomotive force due to fast magnetosonic waves, Eq.(2-11) takes the form as

$$\frac{\partial}{\partial t}\left[\frac{\partial}{\partial x}\left(\rho_0 \frac{\partial \phi}{\partial x}\right) + \frac{\partial}{\partial y}\left(\rho_0 \frac{\partial \phi}{\partial y}\right)\right] - \frac{1}{4\pi}\left[B_{x0}\Delta\left(\frac{\partial A}{\partial x}\right) - \frac{d^2 B_{x0}}{dy^2}\frac{\partial A}{\partial x} + B_n \Delta \frac{\partial A}{\partial y}\right] + g\frac{\partial \rho_1}{\partial y} + 2\rho_0 v_A^2 \frac{\partial^2 I}{\partial x \partial y} = 0, \tag{3-3}$$

where the last term represents the effect of the ponderomotive force, which comes from the $z$-component of curl $\boldsymbol{F}$.

### Ⅲ-2. Wave Kinetic Equation for Fast Magnetosonic Waves

In order to make dicussions self-consistent, we have to consider the wave kinetic equation for fast magnetosonic waves, which describes the wave intensity $I$, interacting with the reconnecting modes. The wave kinetic equation (Sakai and Washimi, 1982) is given by

$$\frac{\partial I}{\partial t} + v_g \frac{\partial I}{\partial x} + \frac{g}{v_g} I + \frac{1}{v_g}\left[\frac{1}{\rho_0}\frac{\partial \hat{p}}{\partial x} - \frac{B_n}{2\pi\rho_0}\frac{\partial^2 A}{\partial x^2} + v_g \frac{\partial^2 \phi}{\partial x \partial y} + \frac{\partial^2 \phi}{\partial t \partial y}\right] I = 0, \tag{3-4}$$

where $v_g$ is the group velocity of the fast waves and $\hat{p}$ the pressure perturbation associated with the reconnecting mode, which is given by

$$\hat{p} = \rho_1 c_s^2. \tag{3-5}$$

The basic equations describing the coupling between the fast magnetosonic waves and the reconnecting modes are Eq.(2-10), (2-12), (3-3) and (3-4).

### Ⅲ-4. Forced Reconnecting Modes due to Fast Waves

If we assume that the external fast magnetosonic waves persist long enough ($> 10^2\,s$) during the interaction with reconnecting modes, we can divide the wave intensity $I$ into two parts,

$$I(x, y, t) = I_0(x) + I_1(x, y, t), \tag{3-6}$$

where $I_0$ is determined from the equation

$$v_g \frac{\partial I_0}{\partial x} + \frac{g}{v_g} I_0 = 0 , \tag{3-7}$$

which gives a solution

$$I_0(x) = I(0) \exp(-gx/v_g^2) . \tag{3-8}$$

$I_1$ represents the perturbation due to the coupling with reconnecting modes. From Eq.(3-8), we find that the wave intensity gradually decreases in the vertical direction, where its characteristic scalelength $\Delta$ is given by $\Delta = v_g^2/g$. If we use $v_g \simeq v_A = 2.10^7\ cm\ s^{-1}$, $g \cong 10^4\ cm\ s^{-2}$, $\Delta$ becomes $\Delta \simeq 4 \times 10^{10}\ cm$, which means that the wave intensity $I_0$ is nearly constant in the prominence, because $\Delta$ is larger than the characteristic height ($5.10^4\ km$) of the prominence. Assuming all perturbed quantities as $f(y)\exp[i(kx - \omega t)]$ and linearizing Eq.(3-4) around $I_0$, we find

$$I_1 = \frac{kI_0}{(\omega - kv_g - i\frac{g}{v_g})\, v_g} \left[ \frac{c_s^2}{\rho_0} \rho_1 - i \frac{kB_n}{2\pi\rho_0} A + \left( v_g - \frac{\omega}{k} \right) \frac{d\phi}{dy} \right], \tag{3-9}$$

where we used Eq.(3-5). As shown later, the real frequency part is approximately given by $\omega \simeq kv_g = kv_A$, which shows that the dominant terms in Eq.(3-9) are the first and the second terms and also the dominant term in the denominator in Eq.(3-9) is the last term. From these considerations and elimination of $I_1$ in Eq.(3-3), we obtain

$$\begin{aligned} &\frac{d^2\phi}{dy^2} - k^2\phi + \frac{\rho_0'}{\rho_0} \frac{d\phi}{dy} + \frac{k}{4\pi\rho_0\omega} \left[ B_{x0} \left( \frac{d^2}{dy^2} - k^2 \right) A - B_{x0}'' A \right] \\ &+ \frac{B_n}{4\pi\rho_0 i\omega} \frac{d^3A}{dy^3} - \frac{B_n k^2}{4\pi\rho_0 i\omega} (1 - 4k\Delta I_0) \frac{dA}{dy} \\ &+ \frac{gk}{i\rho_0\omega^2} \left( 1 - \frac{2c_s^2 v_A^2 k^2 I_0}{g^2} \right) \frac{d}{dy} (\rho_0' \phi) = 0 , \end{aligned} \tag{3-10}$$

where the last two terms shows the modification due to the ponderomotive force of the fast waves.

Here we consider the physical mechanism, why the slowly growing reconnecting modes can be enahnced by the ponderomotive force of the fast waves. We imagine the situation where there occurs weakly unstable reconnecting modes, as shown in Fig. 2 (b). Near the $X$ type-points region the plasma exhibits inflow into the $X$-point, while near the $O$-type region, the outflow occurs. Equation (2-10) shows that density enhancement appears near the $O$-type region, on the other hand the density decreases near the $X$-point. The coupling eq.(3-9) between the reconnecting modes and fast modes indicates that the density increment gives rise to the decrement of $I_1$ and vice-versa, because the dominant term of Eq.(3-9) should be read as $I_1 \simeq i(kI_0 c_s^2/g\rho_0)\rho_1$, which shows that $\rho_1$ and $I_1$ are out of phase with each other. These interactions cause the inhomogeneous distribution of the intensity of the fast mode, which was nearly constant in the prominence. The wave intensity can be enhanced near the $X$-point region. Eventually, the ponderomotive force of the fast mode can drive the plasma vortex motions near the $X$-point shown in Fig. 6.

We have confirmed by numerical calculations that the main term contributing to the stability is the last one in Eq.(3-10), which represents the acceleration effect due to gravity, if the

ponderomotive force does not exist, and furthermore the term including $\partial A/\partial y$ is not essential for the stability problem; it only modifyies the real frequency part.

If we take into account the ponderomotive force, and the intensity $I_0$ exceeds a critical value $I_c$ given by

$$I_c = \frac{g^2}{2 c_s^2 v_A^2 k^2}, \tag{3-11}$$

the sign of the last term in Eq. (3-10) can change, which means that the effective gravity due to the ponderomotive force exceeds the gravity, $g$. It is easily understood that if the net gravity changes sign by the lifting force due to fast waves, the system will be unstable. In order to confirm the above idea, we have changed the sign of gravity in Eq. (3-10) and calculated the growth rate. The growth rate and real frequency versus $B_n/B_\infty$ are shown in Fig. 7, with parameters, $S = 10^3$, $\alpha = ka = 0.5$. From the numerical calculations, we find that the forced reconnecting mode does not depend on $S$, which means that the instability can be driven by the effective accelerating term due to the ponderomotive force. The growth rate $\gamma\tau_A$ is about 0.3 in the region of $E_n \simeq 0(1)$, which means that the typical growing time $\tau$ is about 100 $s$, i.e. very rapid.

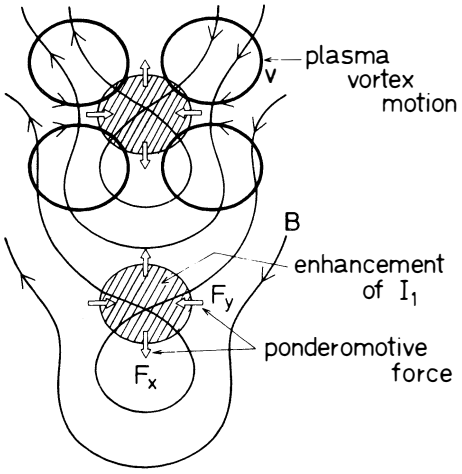


Fig. 6 The plasma vortex motions due to the ponderomotive force of the fast magnetosonic waves.

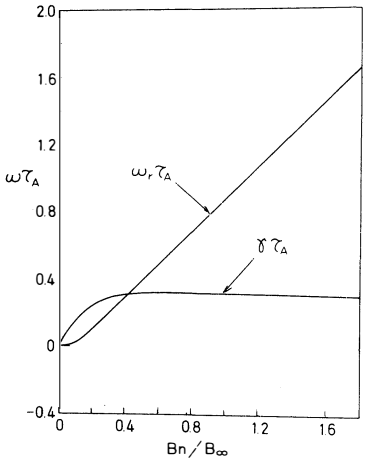


Fig. 7 Growth rate and real frequency of the forced reconnecting mode as a function of $E_n = B_n/B_\infty$ with $ka = 0.5$ and $S = 10^3$.

Another interesting characteristic of this instability appears in its eigenfunction of velocity shown in Fig. 8. The eigenfunction $\phi$ oscillates across the current sheet, which means that the instability creates multiple plasma vortexes across the prominence. Furthermore, fairly broad band waves with shorter wavelength than the width of the prominence can be excited. By making use of quasi-linear approximation, we can estimate the diffusion coefficient $D_\perp$ across the prominence,

$$D_\perp = \sum_{k\omega} \frac{\gamma k^2}{2(\omega_r^2 + \gamma^2)} |\phi_k|^2 . \tag{3-12}$$

We estimate the total mass loss $M_l$ as

$$M_l = \int \rho dx dS = D_\perp \frac{\partial \rho}{\partial x} \Delta t S_0 , \tag{3-13}$$

where $\Delta t$ is the typical growth time, which is taken as $\Delta t \simeq 10^2$ $s$, and $\partial\rho/\partial x \simeq m_i n_0/a = m_i\, 10^{10}/5 \times 10^8 = 20\, m_i$. $S_0$ is the total area, $S_0 \simeq 5 \cdot 10^4 km \times 10^5 km = 5 \times 10^{19}$ $cm^2$. On the

other hand, the diffusion coefficient $D_\perp$ is approximately given by

$$D_\perp \simeq \frac{\gamma}{2\omega_r^2} v_k^2 , \tag{3-14}$$

where we used $\omega_r \gg \gamma$ in the of $E_n \simeq 0(1)$ and $v_k$ is typical random velocity. As $\gamma \simeq 0.3\ \tau_A^{-1}$ and $\omega_r \simeq \tau_A^{-1}$, we find

$$D_\perp \simeq 0.1\, \tau_A\, v_k^2 . \tag{3-15}$$

Observations (Tandberg-Hanssen, 1974) show that prior to a dispersion brusque, the prominence material exhibits increased random motions with velocities $v_k \simeq 30$–$50\ km\ s^{-1}$. If we use this value as $v_k$ in Eq.(2-30), we obtain $D_\perp \simeq 10^{15}\ cm^2 s^{-1}$. The total mass loss $M_l$ is about $10^{38}\ m_i g$, which is about *20 %* of original total prominence mass. Due to the mass loss leading to the unbalance of forces along the vertical direction $[\rho_0 g < (B_n/4\pi)(\partial B_{x0}/\partial y)]$, the prominence may exhibit the observed ascending motion.

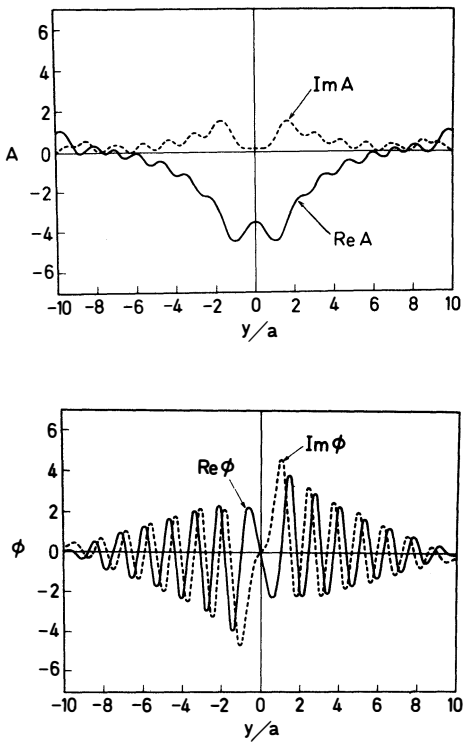


Fig. 8 Eigenmode structures of $A$ and $\phi$ with $S = 10^3$, $E_n = B_n/B_\infty = 0.1$, $ka = 0.5$ and $\omega\tau_A = 0.02078 + 0.1427i$. The oscillating structure of $\phi$ makes a series of vortexes in the magnetic island. The amplitudes of $A$ and $\phi$ are plotted in arbitrary units.

## Ⅳ. DISCUSSIONS AND CONCLUSIONS

We have shown that the current-sheet prominence of Kippenhahn and Schlüter is almost stable against reconnecting modes, however, it becomes suddenly unstable with the time scale of $\tau \simeq 10^2\ s$ by the externally driven nonlinear fast magnetosonic waves. The threshold of fast waves causing forced reconnecting instability is given by Eq.(3-11), which can be estimated as $I_c = 0.5\,(v_A/c_s)^2 (k\Delta)^{-2}$. If we take $v_A/c_s \simeq 10$, and $(k\Delta) \simeq 10^2$, $I_c$ is about $0.5 \cdot 10^{-2}$, which means that if the wave amplitude $\psi = \Delta B/B_0$ of fast waves exceeds $\psi_c = 0.07$, the forced reconnecting mode can be excited by the ponderomotive force of the fast waves.

The first magnetosonic waves with relatively high amplitude $\psi \sim 0.1$ may be excited from other active regions or solar flares. It is interesting to note that such finite amplitude fast magnetosonic waves that excite reconnecting modes are modulational unstable (Sakai, 1983(b)), and decay into slow magnetosonic modes associated with local enhancement of the amplitude. The modulational instability which threshold $\psi_m$ is given by $\psi_m = c_s/v_A \simeq 0.1$ gives rise to more effective interaction between fast waves and reconnecting modes.

Besides the role of fast magnetosonic waves causing the effective acceleration, the increase of supporting magnetic field $B_n$ due to hitting of the foot or whole magnetic field change by a newly emerging magnetic flux nearby may give rise to the ascending acceleration, and in turn there appear forced reconnecting modes.

It is important to consider the nonlinear stage of the forced reconnecting modes, in connection

with plasma heating and particle acceleration mechanism, because as mentioned before soft $X$-rays pictures (Švestka, 1976) show a brightening above the place where the filament just disappeared. In the early stage of the reconnecting instability, many current filaments are produced with currents all in the same direction. Such a system will be unstable against nonlinear coalescence instability (Wu et al., 1980 ; Leboeuf et al., 1981), which leads to intense plasma heating and particle acceleration. It is important to keep in mind that about *10 %* of the magnetic field energy sustaining current filaments can be converted to plasma thermal energy as well as high energy particle acceleration. The nonlinear coalescence instability is thought to an important mechanism for plasma heating after disparition brusque as well as solar flares and $X$-rays brightening in the corona (Tajima et al., 1982).

We have investigated the triggering mechanism of disparitions brusques by fast magnetosonic waves which leads to forced excitation of the reconnecting mode. The reconnecting mode can also be externally driven by finite amplitude shear Alfvēn waves which may originate from the foot of the magnetic field sustaining the prominence. The details of this mechanism will be published elsewhere (Sakai, 1983 (c)

## ACKNOWLEDGMENTS

The one (Sakai) of authors would like to thank S. Migliuolo, C. Hyder, and B. C. Low for their valuable comments concerning the manuscript. He also would like to thank R. M. MacQueen and the staff of the High Altitude Observatory for their hospitality while visiting the Observatory.

A part of the paper has been presented in the 1982 International Conference on Plasma Physics held on June 8-15, 1982 at Göteborg, Sweden.

## REFERENCES

1) Anzer, U. : 1969, Solar Phys. **8**, 37.
2) Dolginov, A. Z., and Ostryakov, V. M. : 1980, Sov. Astron. **24**, 749.
3) Dungey, J. : 1958, Cosmic Electrodynamics, University Press, Cambridge, p. 54.
4) Furth, H. P., Killeen, J. K., and Rosenbluth, M. N. : 1963, Phys. Fluids **6**, 459.
5) Measley, J. N., and Mihalas, D. : 1976, Ap. J. **205**, 273.
6) Hyder, C. L. : 1967, Solar Phys. **2**, 49.
7) Kıppenhahn, R., and Schlüter, A. : 1957, Z. Aztrophys. **43**, 36.
8) Kuperus, M., and Tandberg-Hanssen, E. : 1967, Solar Phys. **2**, 39.
9) Leboeuf, J. M., Tajima, T., and Dawson, J. M. : 1982, Phys. Fluids **25**, 784.
10) Low, B. C. : 1975, Ap. J. **197**, 251.
11) Low, B. C., and Wu, S. T. : 1981, Ap. J. **248**, 335.
12) Lerche, I., and Low, B. C. : 1977, Solar Phys. **53**, 385.
13) Migliuolo, S. : 1982, J. Geophys. Res. **87**, 8057.
14) Milne, A. M., Priest, E. R., and Roberts, B. : 1979, Ap. J. **232**, 304.

15) Nakagawa, Y. : 1970, Solar Phys. **12**, 419.
16) Nakagawa, Y., and Malville, J. M. : 1969, Solar Phys. **9**, 102.
17) Nishikawa, K-I. : 1980, J. Phys. Soc. Japan **48**, 2104.
18) Nishikawa, K-I., and Sakai, J. : 1982, Phys. Fluids **25**, 1384.
19) Pustil'nik, L. A. : 1974, Sov. Astron. **17**, 763.
20) Sakai, J. : 1982 (a), Ap. J. **263**, 970.
21) Sakai, J. : 1983 (b), Solar Phys. (in press)
22) Sakai, J. : 1983 (c), (in preparation).
23) Sakai, J., and Washimi, H. : 1982, Ap. J. **258**, 823.
24) Švestka, Z. : 1976, Solar Flares, Dordrecht, D. Reidel.
25) Švestka, Z. : 1980, Phil. Trans. R. Soc. Lond. **A297**, 575.
26) Tajima, T., Brunel, F., and Sakai, J. : 1982, Ap. J. **258**, L45.
27) Tandberg-Hanssen, E. : 1974, Solar Prominences, D. Reidel Pub. Co.
28) Wu, C. C., Leboeuf, J. N., Tajima, T., and Dawson, J. M. : 1980, PPG-511, Center for Plasma Physics and Fusion Engineering, UCLA.
29) Zweibel, E. : 1982, Ap. J. **258**, L53.

(Received. October 20. 1982)